Research

Application of fallout radionuclide—¹³⁷Cs for estimating soil erosion in steep hillslopes with diverse land use of North-western Indian Himalayas

Suresh Kumar[1] · Anu David Raj[2,3] · Sankar Mariappan[4] · Justin George Kalambukattu[2] · K. R. Sooryamol[4] · R. P. Singh[5] · M. Madhu[4] · N. Karunakara[6]

Abstract

Hilly and mountainous regions are significantly impacted by soil erosion, primarily due to rainfall-runoff processes occurring on the hillslope scale. Assessing soil erosion is crucial for quantifying the loss of soil carbon and nutrients, which diminishes the potential of soil ecosystem services and is critical for mitigating the impacts of climate change on food security. However, the Himalayan landscape poses serious challenges for assessing soil erosion due to its steep and rugged terrain, which hinders the use of conventional and modelling methods. The fallout radionuclide—^{137}Cs has been extensively utilized as an environmental marker for investigating soil redistribution processes. Despite its potential, there is a notable lack of ^{137}Cs-based soil erosion studies in the Himalayan region. In this context, we assessed the applicability of the fallout radionuclide—^{137}Cs method in quantifying soil erosion rates and identifying erosion hotspots on two hillslopes of the Higher Himalayas. On the hillslope scale, we observed that soil erosion rates vary based on slope gradient and land use/land cover. Forested areas exhibited the lowest soil erosion rates compared to cultivated areas, while flat hillslope positions experienced lower erosion rates than steeper positions. The average net erosion rate for the Harsil hillslope varied among different hillslope positions, ranging from − 2.9 to − 15.6 t ha^{-1} yr^{-1}. Similarly, in the Gangnani hillslope, the net erosion rates varied across different positions, ranging from − 5.6 to − 39 t ha^{-1} yr^{-1}. Our findings confirm that the middle and lower hillslope positions are the most critical source areas with higher soil erosion rates, while hillslope positions with forest cover demonstrate the lowest erosion rates, identified as helpful in controlling soil erosion. The study has demonstrated the applicability of FRN as a soil erosion measurement method in the complex, rugged, and steep terrain of the Himalayas, highlighting the need for targeted conservation efforts to mitigate soil erosion and preserve ecosystem integrity.

Keywords Hillslope · Himalayas · Radiocesium · Soil erosion · Soil redistribution

✉ Anu David Raj, anudraj@iirs.gov.in; anudraj2@gmail.com | ¹Agriculture, Forestry and Ecology Group, Indian Institute of Remote Sensing (IIRS), Indian Space Research Organisation (ISRO), Dehradun, India. ²Agriculture and Soils Department, Indian Institute of Remote Sensing (IIRS), Indian Space Research Organisation (ISRO), Dehradun, India. ³Forest Research Institute (FRI), deemed to be University, Dehradun, India. ⁴Indian Institute of Soil and Water Conservation (IISWC), Indian Council of Agricultural Research (ICAR), Dehradun, India. ⁵Indian Institute of Remote Sensing (IIRS), Indian Space Research Organisation (ISRO), Dehradun, India. ⁶Centre for Advanced Research in Environmental Radioactivity (CARER), Mangalore University, Mangalore, India.

Discover

1 Introduction

Soils play a vital role in supporting life on Earth (life on land—SDG 15) and are indispensable for the functioning of ecosystems, as well as for climate change mitigation and adaptation (climate action—SDG 13). Soil erosion caused by water poses a significant threat to soil functionality, resulting in a decrease in soil quality and sustainable crop production [1]. In the hilly and mountainous regions, soil erosion is accelerated by unsustainable human activities (intensive agriculture and deforestation), steep slopes, and high-intensity rainfall (climate change). Soil erosion can significantly contribute to the increased release of stored soil carbon, leading to CO_2 emissions. This influences global warming and climate change, ultimately affecting ecosystem services [2]. Consequently, it evolves into a major global agro-ecological concern that influences socio-economic and political decision-making. Hence, appropriate conservation measures and land use planning need to be implemented to mitigate the adverse impacts resulting from it.

The Himalayan region is commonly known as Asia's water reservoir, with approximately 1.5 billion individuals inhabiting the river basins downstream from this mountain range [3]. However, the Himalayas, being young and fragile mountain range composed of weak and unstable formations, are particularly vulnerable to soil erosion [4]. Inadequate land management practices further exacerbate soil erosion in the hilly and rugged regions of the Himalayas [5]. Significantly, the Himalayas have been reported to exhibit exceptionally high soil erosion rates, ranging from 20–25 t ha^{-1} yr^{-1} to reaching as high as 92 t ha^{-1} yr^{-1} in various regions [6–9]. Thus, rivers in this region transport substantial quantities of sediments and soil nutrients to reservoirs and oceans [10]. Numerous global-scale studies [11, 12] have also underscored the Himalayas as a major global hotspot of soil erosion. Moreover, future climate change scenarios predict increased rainfall, which may further exacerbate soil erosion in the Himalayas [7, 13].

The sustainable utilization of mountain resources depends on the conservation and responsible management of soil and water resources [14]. Reliable information on soil erosion rates and a comprehensive understanding of erosion processes are prerequisites for developing effective natural resource management plans. However, the absence of gauged watersheds poses significant challenges in comprehending hydrologic processes [15]. In addition, modelling methods suffer from limited resolution and static observations, impeding spatial assessment and the identification of erosion hotspots [12, 16]. Furthermore, they have several limitations in terms of operational problems and the substantial need of resources for their spatial and temporal coverage [17]. The Himalayan region has been largely ignored in measurement studies due to its rugged and inhospitable terrain conditions [13, 18]. This may have caused a significant lack of field measurement studies on soil erosion in the Himalayan region [19]. The complex, rugged, non-uniform steep slopes of the Himalayas make it difficult to conduct runoff/erosion plot studies. Modeling could fail on slopes greater than 50%, reducing the reliability of conventional and modeling methods in the Himalayas. According to Wischmeier and Smith [20], the USLE model stipulates that the calculation of the LS factor relies on slopes between 2 and 18%, as well as plot/field sizes ranging from 30 to 300 feet. The accuracy of these data relationships beyond these thresholds has not been confirmed through direct soil loss measurements. Estimating field erosion rates using sediment concentrations might lead to underestimation due to variable sediment trapping between the field and the riverbed. Furthermore, if riverbank erosion significantly contributes to sediment supply in the river, there's a chance that sediment yields could overestimate actual erosion rates on the fields [11]. The most dependable relationships with measured sediment yields are predominantly associated with catchment sizes featuring homogeneous land use and soil types [11]. Many methods limit estimation to a maximum slope angle of 50% (26.6 degrees) [21], and LS factors exceeding this threshold introduce uncertainty into soil erosion predictions. Traditional methods for assessing soil erosion, including volumetric techniques, erosion plots, hydrological measurements, and geodetic surveys, are applied to various erosion processes and encompass different spatial and temporal scales. However, these methods often face significant limitations that affect the accuracy of the data collected [22]. Thus, Kumar et al. [23] suggested that in steep sloping hilly, and mountainous regions fallout radionuclides (FRNs) could be a comparatively reliable alternative for soil erosion assessments. It is considered highly effective in extreme topographic and climatic conditions, which restricts the applications of conventional methods [24, 25].

Over the past few decades, FRNs including artificial radioisotopes like ^{137}Cs and $^{239+240}$Pu, natural fallout of ^{210}Pb, and cosmogenic ^{7}Be have been extensively employed as soil tracers. They have been helpful in evaluating soil erosion rates across various environmental conditions [24, 26, 27]. The ^{137}Cs radioisotope is the most widely used and validated method to quantify soil erosion rates for the medium term [28, 29] and is a man-made isotope with a half-life of 30.2 years. Yamagata et al. [30] made one of the earliest efforts to utilize cesium in the study of soil erosion and its movement. The use of FRN activity monitoring has been acknowledged as an effective method for investigating how soil is redistributed throughout the landscape [31]. It originated in the environment because of atmospheric thermonuclear weapons

testing conducted during the 1950s and 1960s [28]. The use of ^{137}Cs as a tracing agent relies on the assumption that it is uniformly distributed across the landscape and quickly and strongly binds to specific components, particularly clay particles and organic substances like humus. Additionally, it exhibits resistance to being carried deeper into the soil or absorbed by plants. Consequently, ^{137}Cs is primarily redistributed in association with the physical movement of soil particles. FRN also aids in comprehending erosion processes by providing insights into the time of deposition of specific FRN, and this analysis can be conducted within a single sampling campaign. There are various models available for the conversion of areal activity into erosion rates ranging from simple proportional models to complex mass balance models [32]. Most recently, a new model named Modelling Deposition and Erosion rates with Radionuclides (MODERN) has been introduced. This model takes into account the exact depth distribution of any FRN at a reference site and enables customization to suit specific site conditions [33] and employed by several other studies across the globe and found efficient [34]. While Parson and Foster [35, 36] have raised concerns about the reliability of ^{137}Cs, although adherence to the underlying assumptions, meticulous parameterization, and optimal sampling strategy can provide a long way in resolving these issues [28, 29, 37]. Furthermore, the continued global use of ^{137}Cs in soil erosion and sediment fingerprinting research [38] demonstrates its usefulness. Notably, it can avoid the need for time-consuming and expensive methods typically required for long-term site monitoring [26, 28, 29] which is impossible in the complex terrain of the Himalayas.

In the higher Himalayas, there is a significant lack of field erosion measurement; only predictions or potential assessments of soil erosion rates have been made [19]. Previous studies on soil erosion in the Himalayan region have primarily relied on approximations based on sediment yield at the watershed or catchment scale, or they have used erosion models to make predictions. Also, there is a significant lack of reliable information regarding soil erosion rates using FRN—^{137}Cs [38], with only a few numbers of studies were conducted in the foothills, lower Himalayan regions, and north-eastern part of India (Meghalaya) [9, 39, 40]. Notably, there is a significant lack of such studies in the steep sloping higher Himalayas. Mariappan et al. [40, 41] have underscored the necessity, potential, and existing gap in the application of fallout radionuclides for the Indian sub-continent and Indian Himalayas [23]. The present study aims to quantify soil erosion rates on two typical hillslopes characterized by steep topography in the Higher Himalayas. Specifically, the study seeks: (i) to characterize the depth distribution of ^{137}Cs in the higher Himalayas, (ii) to quantify the long-term average soil erosion rate in steep, complex landscapes, and (iii) to identify critical hillslope positions prone to soil erosion.

2 Materials and methods

2.1 Study area

The Himalayan landscape consists of mosaics of complex hillslopes. Two typical hillslopes representing the higher Himalayas were selected to quantify erosion rates over the hillslope. The higher Himalayas mark the region with the highest peaks of the Himalayas, comprising a thickness of 10–15 km of Precambrian crystalline rocks that have been uplifted and intruded by granites, some of which are tertiary in age [42]. The region mainly consists of metamorphic schist rock types. Soils are dominantly sandy loam type and belong to sub-group of Typic Dystrudepts [43]. The climate is classified as warm and temperate according to the Köppen Climate Classification (Cwb) [44]. The area also receives seasonal snowfall during winter.

2.2 Harsil (H1)

The hillslope is situated at 31° 01′ 55.4″ latitude and 78° 44′ 26.9″ longitude in Harsil, Uttarkashi, Uttarakhand, India (Fig. 1). Agriculture serves as the primary occupation for the local population. The annual average precipitation ranges from 1000 to 1350 mm (1951–2021) based on IMD Gridded data, with approximately up to 60–70% occurr during the monsoon season from June to September [45]. The ridge (HS1) of the hillslope is predominantly covered with cropland characterized by high soil depth. These terraced croplands are rain-fed and cultivated with *Phaseolus vulgaris* (red kidney beans) (*Rajma*) and Potato (*Aloo*). These terraces are almost flat, lacking embankments at the field boundaries and sloping outward. In the upper hillslope (HS2), dense coniferous forests dominate, primarily covering Deodar (*Cedrus deodara*) and Himalayan Spruce (*Picea smithiana*), with a moderately deep soil depth. The middle to lower sections of the hillslope are occupied by terraced Apple orchards (HS3 & HS4), ranging from very deep to deep soil profiles, respectively. In HS3, the terraces were wide and outward sloping with deep soil, whereas in HS4, the terraces were narrow, closely spaced, and located on steep slopes, with an outward slope direction. Further down, in the valley hillslope (HS5), mixed forests (*Cedrus*
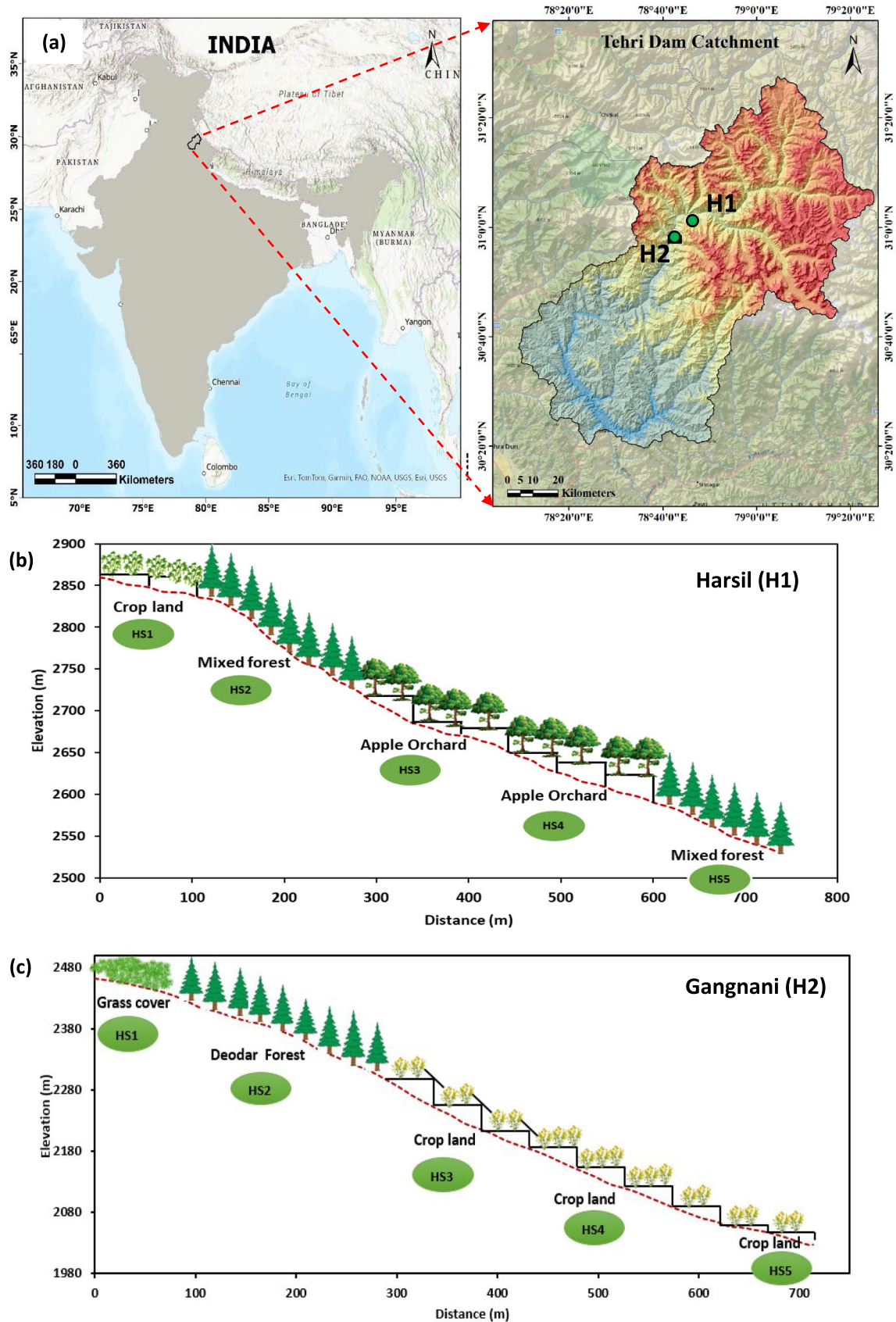
Fig. 1 (**a**) Location of the study area hillslopes—(**b**) Harsil (H1), and (**c**) Gangnani (H2)

deodara and *Picea smithiana*) with moderate soil depth prevail. Cropping is limited to a single season due to snow cover for the remainder of the year. Traditional animal-drawn plough tillage has been practiced in this area for over a century with plough layer depths ranging from approximately 15–20 cm.

2.3 Gangnani (H2)

This hillslope is located at 30° 54′ 08″ latitude and 78° 41′ 06″ longitude at Gangnani, Uttarkashi, Uttarakhand, India (Fig. 1). The yearly average precipitation amounts to 1367 mm, with around 70% of it falling during the monsoon season, which occurs from June to September (Supplementary Fig. 1 & 2). The ridge (HS1) of the hillslope is covered with grasses and shrubs characterized by medium soil depth. The upper hillslope (HS2) was characterized by dense coniferous forests (*Cedrus deodara and Picea smithiana*) and has moderately deep soil. The middle to lower hillslope is terraced cropland (HS3 & HS4) with varying soil depths, ranging from shallow and deep respectively. At mid hillslope (HS3), terraces were damaged and slightly outward sloping with broken stone patches on the riser of the terraces. The terraced fields at HS4 were comparatively wider than the HS3 position, with stone patching on riser and slight outward slope. The lowest hillslope position (HS5) farmers do cultivation rarely. These terraced croplands were rain-fed and cultivated with beans/ amaranths during the monsoon season at the middle hillslope position. In the lower hillslopes, amaranthus and *Phaseolus vulgaris* (red kidney beans) are cultivated during the monsoon season, followed by mustard in the winter (rabi) season (Supplementary Fig. 3). Animal-drawn plough tillage were being practiced over a century, with a plough layer depth ranging from approximately 15–25 cm.

2.4 Soil sampling

The hillslopes were selected based on reconnaissance field surveys using remote sensing data and GIS tools, ensuring its precise representation of the region in terms of climate, topography, soil, and land use/land cover. The study employed a simple transect sampling strategy, assuming lateral uniformity across the slope gradient in the distribution of ^{137}Cs, while anticipating non-uniformity along the transect concerning topography and land use/land cover. This method is particularly suitable for steep and uniform slopes, where a single transect can effectively capture the variability of ^{137}Cs inventories. The transect was aligned along the axis from the highest to the lowest hillslope positions, comprising a sequence of sampling points from the ridge/hilltop to the valley [40, 46, 47]. The hillslopes were comprising of both forested and terraced cultivated areas. The construction of terraces predates the main period of ^{137}Cs fallout, which occurred during 1950s and the 1960s. Soil sampling along the transects of the typical hillslopes were conducted during March 2022 and 2023. The selected hillslope direction was in north for Harsil (H1) and northwest for Gangnani (H2). Sampling sites were located at intervals of approximately 150–200 m along transects of 750 (H1) and 730 (H2) meters in length, corresponding to the hillslope elements (Fig. 1). The spacing between sampling points varied depending on the length of the slopes in forested areas and the terrace width in the cropland areas. To ensure representative sampling sites, the sites were carefully selected to reflect the pattern of soil redistribution, influenced by water flow direction, slope steepness, and variations in land use/land cover. At each hillslope element/position, one pit was selected for soil sampling, representative of the hillslope position. Samples were collected from the center of the terraced fields to ensure their representativeness.

Soil samples were collected from different depths at 15 cm intervals along three sides of each soil profile (a pit of 1 m^3), with three replications taken for each layer (Fig. 2) [40]. To reduce uncertainty in the reference site, soil samples were selected from each of the three faces of multiple pits. We used six to nine replications at the reference site for each layer and samples were taken from two- three pits (n = 6–9). Various studies have used six to nine replications per single layer at the reference site [48–50]. The slope angles of the reference site ranged < 2 degrees and were covered with grasses and shrubs, exhibiting minimal erosion and no visible signs of surface erosion. Soil samples were collected to a maximum depth of 1 m or until reaching bedrock or parent material, using stainless steel sampling boxes with average dimensions of 0.10 × 0.10 × 0.05 m, 0.15 × 0.10 × 0.05 m, and 0.20 × 0.10 × 0.05 m. To assess variations in radionuclide contents at different depths within the soil profile, an entire section of the soil profile within a metal box, commonly referred to as a box-monolith core, was employed. Then, the perpendicular surface of the soil profile was exposed. A metal box section was then carefully inserted into the exposed surface (using a wooden block and hammer) until it aligned evenly with the adjacent surface. Subsequently, the metal box was removed from the profile, and soil samples were collected and placed into appropriately labeled polythene bags (Fig. 2) [40, 51]. A detailed soil sampling methodology adopted can

Fig. 2 Pit-based depth-incremental procedure followed for soil sampling

be found in Mariappan et al. [40]. A total of 135 soil samples were collected from the hillslopes and analyzed for ^{137}Cs concentration, as well as various physico-chemical properties of the soil.

2.5 Soil analysis

2.5.1 Physio-chemical analysis of soils

Soil samples were collected from both forested and cropland areas in the hillslope positions along the transect. The sampling involved obtaining samples at different depth intervals, specifically at 0–15 cm and 15–30 cm. Once collected, the samples were air-dried, disaggregated, and sieved through a < 2 mm sieve. Soil physio-chemical parameters such as soil texture, bulk density, pH, electrical conductivity (EC), and soil organic matter contents were analyzed at the Central Analytical Lab (CAL), Indian Institute of Remote Sensing, Dehradun. Supplementary Table 1 provides further details and information on the methods used to analyze the physico-chemical properties of the soils.

2.5.2 Gamma spectroscopy

Gamma spectroscopy was employed to determine the activity concentrations of ^{137}Cs in soil samples. A p-type broad energy high purity germanium (HPGe) detector with a carbon composite window (BEGE-5030, Canberra Industries Inc., USA), available at the Centre for Advanced Research in Environmental Radioactivity (CARER), Mangalore University, was utilized for the analysis. The Gamma Spectrometer, along with efficiency calibration details, has been previously documented [52]. The soil samples, each weighing 250 g, were subjected to a counting duration of 60,000 s. The activity concentration was then estimated based on the 662.6 keV gamma emission from ^{137}Cs, and the calculation followed equation provided in Supplementary file. To determine the ^{137}Cs content for each layer in the soil profile, measured in Bq m^{-2}, the mass of the fraction less than 2 mm and the cross-sectional area of the sampling device were employed in the calculation.

2.6 Measurement and modelling of FRN-^{137}Cs reference inventory

The accurate assessment of the reference inventory is essential for quantifying soil erosion and deposition rates using ^{137}Cs measurements. Identifying a reference site with minimal erosion or deposition in the steep and mountainous terrain of the Himalayas is a major challenge. In this study, the reference site was identified at the ridge or hilltop position with the lowest possible slope (0–2 degrees). The dependability of the measured reference value of the ^{137}Cs inventory can be assessed by the global reference model [9]. We used various methods [53–56] that are available to estimate the reference inventory.

2.7 Conversion of ^{137}Cs inventories to soil redistribution rates

The quantification of erosion and deposition rates along the hillslope transect relies on comparing the measured ^{137}Cs inventory to a reference inventory. Various relationships are available for obtaining quantitative assessments of soil erosion and/or deposition using ^{137}Cs measurements. In ploughed soils, where ^{137}Cs is mixed with the ploughed or cultivated layer, the depth distribution of ^{137}Cs in the soil profile differs significantly from that observed in undisturbed soils. In stable undisturbed soils, the depth distribution of ^{137}Cs typically follows an exponential decrease with depth, and this pattern can be effectively characterized using the profile distribution model [57]. Modelling Deposition and Erosion rates with RadionNuclides (MODERN) model [33] were employed to convert the measured ^{137}Cs inventories into soil erosion and deposition rates for ploughed (cropland) and un-ploughed (forest land) soils.

2.7.1 Modelling Deposition and Erosion rates with RadionNuclides (MODERN)

The MODERN model offers adaptability to specific site conditions and considers the specific depth distribution of any Fallout Radionuclide (FRN) at the reference site. The depth-wise distribution of the reference profile was used to adapt and simulate the erosion/deposition from the hillslope. To simulate soil erosion values in terms of length unit or mass per unit area per year, MODERN requires the mass depth and areal activity of ^{137}Cs. Unlike other models, the MODERN does not necessitate a transect sampling approach and can efficiently execute even when the sampling points are spatially scattered.

The model attempts to determine the level x* (in cm) between x* and x*+d (in cm), where the total FRN inventory of the sample site, Inv, is equal to the sum of all Invinc values of the reference site. Consequently, x* must satisfy the following equation [33]:

$$\int_{x^*}^{x^*+d} g(x)dx = Inv$$

To explore all potential solutions, several simulated layers are incorporated both below and above the reference profile, to evaluate potential soil erosion or aggradation. The integral function S, describes the newly simulated depth profile, where:

$$S(x) = \int_{x^*}^{x^*+d} g(x\prime)dx\prime$$

The distribution function g(x)'s antiderivative (primitive) function G can be utilized to solve the function S, as demonstrated below:

$$S(x) = G(x + d) - G(x)$$

The results provided by MODERN are given in centimeters of soil losses or gains. The following equation can be used to convert Y in t ha^{-1} yr^{-1} to annual soil erosion or aggradation:

$$Y = 10 \times \frac{x^*.xm}{d.(t_1 - t_0)}$$

where xm is the mass depth (kg m^{-2}) at the sampling site, d is the total depth measured, t1 is the sampling year (yr), and t0 (yr) is the reference year.

3 Results and discussion

3.1 Physicochemical characterization of soils

The typical hillslope was sub-divided into five segments, including the ridge/hilltop, upper, middle, lower, and valley hillslope positions, and their physio-chemical characterization of soils is provided in Table 1. Soils in the Harsil (H1)

Table 1 Distribution of soil physio-chemical properties (mean ± SD; n = 3)

	Depth (cm)	Sand (%)	Silt (%)	Clay (%)	Bulk density (g cm^{-3})	pH	Electrical conductivity (dS/m)	Organic matter (%)
Harsil (H1)								
Reference	0–15	30.00 ± 5.29	50.61 ± 5.03	19.39 ± 1.50	1.27 ± 0.04	4.82 ± 0.39	0.09 ± 0.07	3.82 ± 0.49
	15–30	28.67 ± 2.83	51.28 ± 2.00	20.05 ± 1.15	1.27 ± 0.02	5.00 ± 0.46	0.06 ± 0.01	3.02 ± 1.02
Ridge	0–15	43.15 ± 2.13	33.33 ± 3.06	23.52 ± 3.05	1.28 ± 0.29	4.82 ± 0.17	0.09 ± 0.02	3.36 ± 0.37
	15–30	44.48 ± 3.05	22.43 ± 5.80	33.09 ± 3.00	1.16 ± 0.1	5.07 ± 0.23	0.06 ± 0.01	2.79 ± 0.43
Upper	0–15	53.33 ± 0.00	33.20 ± 1.13	15.20 ± 1.06	0.90 ± 0.18	5.69 ± 0.03	0.17 ± 0.02	5.47 ± 0.98
	15–30	53.33 ± 1.15	28.67 ± 1.15	18.00 ± 0.00	1.06 ± 0.00	5.58 ± 0.02	0.13 ± 0.00	4.08 ± 0.63
Middle	0–15	55.72 ± 1.41	26.84 ± 1.41	17.44 ± 0.00	1.01 ± 0.70	5.00 ± 0.26	0.09 ± 0.03	3.43 ± 0.52
	15–30	59.72 ± 7.44	22.84 ± 1.41	17.44 ± 0.00	1.10 ± 0.73	5.08 ± 0.29	0.07 ± 0.02	2.69 ± 0.18
Lower	0–15	58.72 ± 6.52	28.85 ± 7.25	12.43 ± 0.74	0.94 ± 0.03	5.08 ± 0.06	0.09 ± 0.04	3.36 ± 0.37
	15–30	58.72 ± 8.16	28.19 ± 8.92	13.09 ± 1.01	1.16 ± 0.05	4.89 ± 0.35	0.07 ± 0.00	3.05 ± 0.18
Valley	0–15	51.28 ± 2.00	38.00 ± 2.00	10.72 ± 0.00	0.76 ± 0.09	5.86 ± 0.19	0.18 ± 0.00	4.17 ± 1.84
	15–30	70.28 ± 1.41	21.00 ± 1.41	8.72 ± 0.00	1.23 ± 0.03	5.72 ± 0.21	0.05 ± 0.03	3.42 ± 0.87
Gangnani (H2)								
Reference	0–15	57.89 ± 3.06	34.00 ± 4.00	8.11 ± 1.15	1.01 ± 0.07	4.04 ± 0.18	0.27 ± 0.06	2.13 ± 0.19
	15–30	59.89 ± 1.15	34.67 ± 1.15	5.44 ± 0.00	1.04 ± 0.03	4.32 ± 0.32	0.16 ± 0.05	1.88 ± 0.10
Ridge	0–15	61.89 ± 6.43	32.67 ± 4.62	5.44 ± 2.00	1.02 ± 0.02	4.65 ± 0.21	0.05 ± 0.02	1.05 ± 0.05
	15–30	61.23 ± 3.06	31.33 ± 1.15	7.44 ± 2.00	1.12 ± 0.08	4.77 ± 0.18	0.04 ± 0.00	0.61 ± 0.24
Upper	0–15	62.56 ± 5.29	32.00 ± 5.29	5.44 ± 0.00	0.87 ± 0.04	5.23 ± 0.29	0.29 ± 0.09	4.70 ± 0.58
	15–30	63.89 ± 4.16	31.33 ± 4.62	4.77 ± 1.15	1.05 ± 0.12	5.40 ± 0.40	0.11 ± 0.03	2.68 ± 0.60
Middle	0–15	57.89 ± 3.06	36.00 ± 4.00	6.11 ± 1.15	1.10 ± 0.03	5.15 ± 0.20	0.32 ± 0.11	0.96 ± 0.62
	15–30	54.56 ± 4.00	38.67 ± 4.16	6.77 ± 1.15	1.17 ± 0.02	5.51 ± 0.09	0.24 ± 0.21	0.46 ± 0.36
Lower	0–15	48.13 ± 1.41	40.00 ± 3.46	11.87 ± 2.67	1.02 ± 0.06	4.63 ± 0.25	0.66 ± 0.06	3.66 ± 0.32
	15–30	47.47 ± 3.76	40.67 ± 1.15	11.87 ± 2.67	1.08 ± 0.07	5.00 ± 0.32	0.28 ± 0.09	2.54 ± 0.30
Valley	0–15	47.28 ± 3.46	40.67 ± 1.15	12.05 ± 3.06	0.98 ± 0.00	4.32 ± 0.24	0.73 ± 0.08	3.44 ± 0.27
	15–30	43.28 ± 3.46	44.00 ± 5.29	12.72 ± 2.00	1.09 ± 0.07	4.96 ± 0.45	0.03 ± 0.13	2.28 ± 0.63

hillslope, ridge, and reference location exhibited a higher clay percentage compared to other hillslope positions. Soils in the Gangnani (H2) hillslope range from predominantly sandy loam at the upper hillslope to loam at the lower hillslope. The textural composition of the soil was observed to vary significantly from the ridge to the valley hillslopes, with a notable increase in silt and clay content, accompanied by a decrease in sand content. It was anticipated that the larger particle size fractions of the deposited soil would decrease compared to the source soil. This is because larger particles typically have a larger shear stress threshold and are less susceptible to erosion [58]. The soils were highly acidic and non-saline in nature. The pH ranged from 4.0 to 5.9, while the EC ranged from 0.05 to 0.73 dS m^{-1} in the surface soils of both hillslopes. The acidic nature of the soils may be attributed to the release of organic acids resulting from the decomposition of high organic matter content present in the soils [59]. The electrical conductivity (EC) exhibited a decreasing trend as soil depth increases, which could be associated with nutrient leaching and its accumulation in lower soil layers [60]. The bulk density of soils ranged from 0.76 (forest cover) to 1.28 g cm^{-3} (cropland) in the surface and sub-surface layers. In the surface soil, soil organic matter ranged from 0.96 to 5.5%, whereas subsurface soil had 0.46 to 4.1%. Overall, higher organic matter was found in the Harsil (H1) hillslope than in Gangnani (H2), as it were located in a cooler and higher altitude region. Elevation and temperature affect organic matter decomposition, with higher elevation and lower temperature favoring slower decomposition [61, 62]. The low bulk density in the forest soil, [63] could be attributed to factors such as active bioturbation, the buildup of organic matter, and the cycles of thawing and freezing. Additionally, the local vegetation in the area plays a vital role in controlling the physio-chemical properties of the soil, leading to enhancements in soil structure, hydrologic properties, and aeration. The variability in soil physical and chemical properties associated with topography, land use/land cover, and soil erosion processes across the hillslopes.

3.2 Vertical distribution of ^{137}Cs at reference sites

The depth distribution profiles of ^{137}Cs exhibited a decreasing exponential pattern ($r^2 = 0.92$) (Fig. 3), with the highest concentration of ^{137}Cs retained in the surface and subsurface layers of 0–30 cm (98.8%) and 30–45 cm (1.2%), respectively, in the Harsil (H1) hillslope. Similarly, ^{137}Cs showed a decreasing exponential shape ($r^2 = 0.96$) (Fig. 4), with the maximum amount of ^{137}Cs retained in the surface and subsurface layers of 0-30 cm (96.6%) and 30–50 cm (2.8%) in the Gangnani (H2) hillslope. The exponential distribution of ^{137}Cs ratifies the reference site is suitable. The reference site measured with the highest concentration of ^{137}Cs at 24.5 ± 4.5 Bq kg^{-1}, and at 21.7 ± 1.6 Bq kg^{-1} for H1 and H2, respectively. Similarly, Foucher et al. [64] reported an average reference ^{137}Cs activity of ~ 20 Bq Kg^{-1} at 30–40° latitude. Prokop and Poreba [9] also reported that in Shillong (North-east Himalayas), the total ^{137}Cs activity in soil was approximately 20 Bq kg^{-1}. (decay corrected to 2022). Most of the vertical translocation of ^{137}Cs in these profiles can be attributed to the illuviation of clay associated with soil organic carbon and high rainfall, as well as downward movement via macropores [9]. The observed depth distribution of ^{137}Cs were corresponded with findings
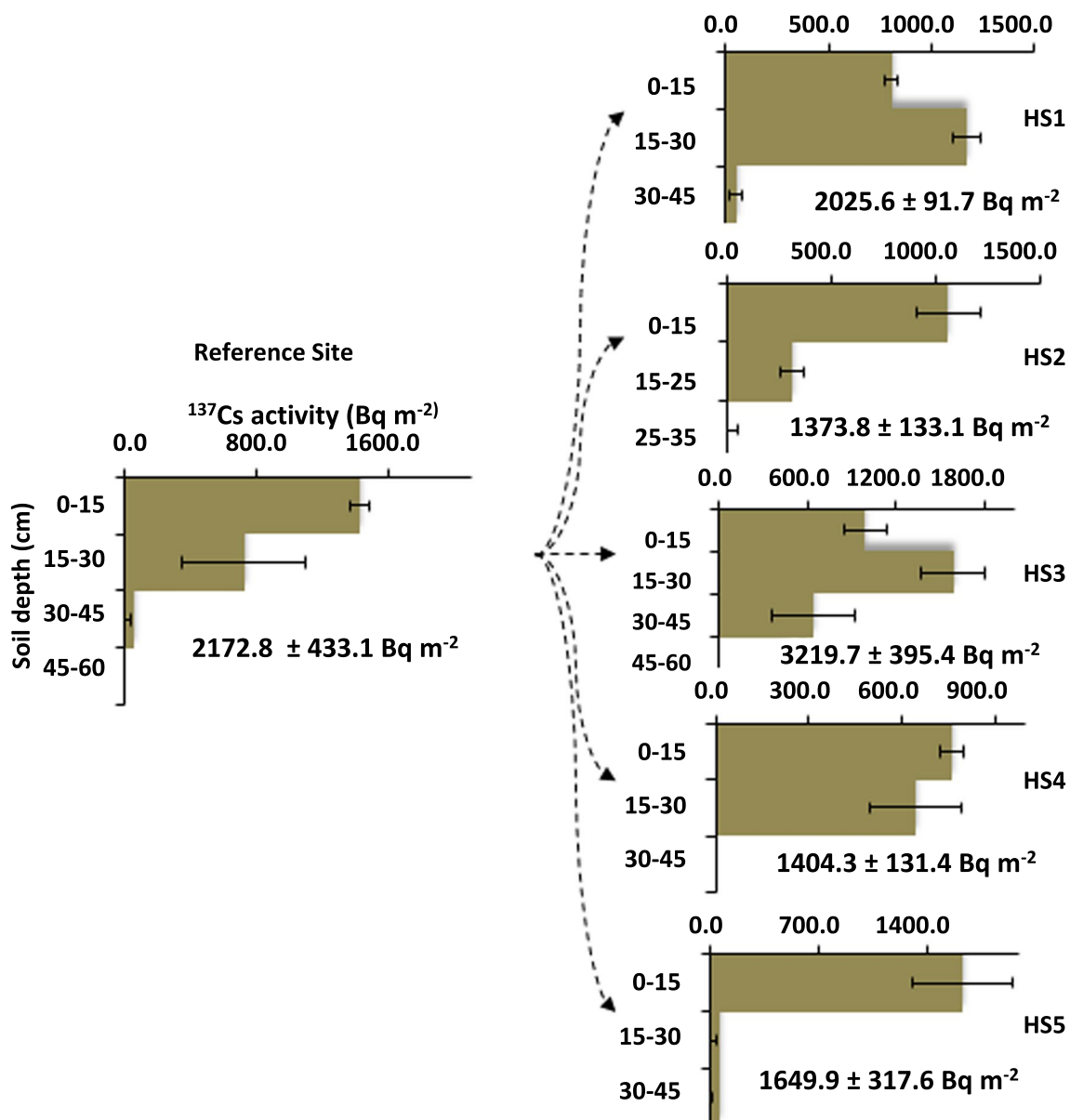
Fig. 3 Vertical distribution of ^{137}Cs in reference points and different hillslope positions of Harsil (H1)
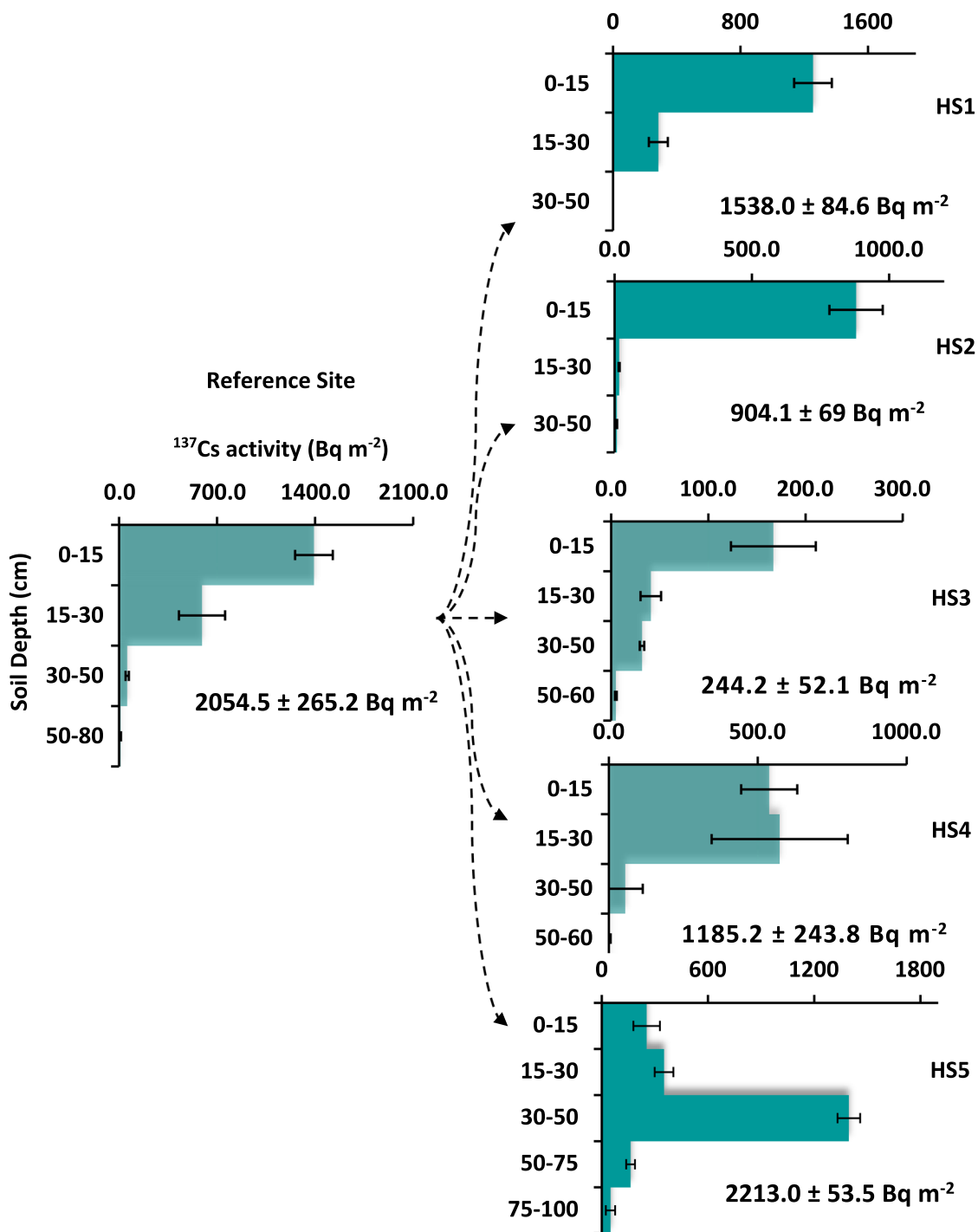
Fig. 4 Vertical distribution of ^{137}Cs in reference points and different hillslope positions of Gangnani (H2)

of other studies. For instance, a significant portion of the total ^{137}Cs inventory was concentrated within the top 30 cm in the Himalayan foothills [40], and up to 35 cm in the Nepal Himalayas [65]. These patterns were consistent with observations from various regions [66]. According to a review by Jagercikova et al. [67], the depth of maximal cesium penetration ranged from 12 to 60 cm. The migration rate of ^{137}Cs is significantly higher in soils rich in soil organic matter and lower in soils with less organic content [67]. In our study, ^{137}Cs was found at depths of up to 30–45 cm, with the majority (96.6–98.8%) found within the top 30 cm.

3.3 Vertical distribution of ^{137}Cs at the sampled sites

In the Harsil (H1) hillslope, the depth distribution profiles of ^{137}Cs along the ridge (HS1), upper (HS2), lower (HS4), and valley (HS5) hillslopes were similar to profiles typically found in un-ploughed and ploughed soils [67], showing an exponential decrease with depth. The ^{137}Cs activities were detected at HS1 (12.6 ± 0.2 Bq kg^{-1}), HS2 (8.7 ± 0.9 Bq kg^{-1}), HS3 (25.4 ± 3.9 Bq kg^{-1}), HS4 (12.1 ± 0.6 Bq kg^{-1}), and HS5 (25.5 ± 6.7 Bq kg^{-1}). In the cropland area (HS1), ^{137}Cs activity was predominantly concentrated (~ 40% and 58%) in the top 15 cm and 30 cm of the soil profile, respectively. In forested sites (HS2 & HS5), 77% and 97% of the ^{137}Cs were found in the top 15 cm, respectively, which is higher than the activity observed in cultivated sites. The middle (HS3) hillslope, characterized by a concave shape with a low slope, exhibited higher ^{137}Cs concentration, with 31%, 49%, and 20% in the depths of 0–15 cm, 15–30 cm, and 30–45 cm, respectively. A comparison with the vertical distribution at the reference site suggests that the top 15 cm of soil in HS3 was deposited from the upslope area. HS4 exhibited an eroded phase, with ^{137}Cs distributed almost equally in the surface and subsurface layers, accounting for 54% and 46%, respectively. In HS5, majority found in surface soils with high amount of coarse fragments was observed. The variation in the depth distribution profiles of ^{137}Cs along the transects indicates variations resulting from changes in land use, topography, soil texture, and stoniness.

In Gangnani (H2) hillslope, significantly higher ^{137}Cs activities were found at HS1 (13.3 ± 0.4 Bq kg^{-1}) and HS2 (12.4 ± 0.6 Bq kg^{-1}), while HS3 (2.3 ± 0.2 Bq kg^{-1}) exhibited lower activity compared to HS4 (11.8 ± 2.1 Bq kg^{-1}) and HS5 (16.8 ± 1.2 Bq kg^{-1}). Li et al. [68] also found that the distribution of ^{137}Cs varies across different hillslope positions. Xinbao et al. [69] found no ^{137}Cs activity in the Loess Plateau on slopes ranging from 100 to 173.20%. However, we found 12.4 Bq Kg^{-1} of ^{137}Cs activity at a steep slope (100–119.17%) with forest cover. ^{137}Cs (~ 97%) is mainly found in the top 15 cm of the soil profile in HS2 (forest), and it translocated downward to a depth of 50 cm ($r^2 = 0.85$). In the cropland (HS3), ^{137}Cs activity was largely (~ 87%) concentrated in the top 30 cm of the soil profile. The ^{137}Cs inventory was maximum within the top 15 cm of the soil and then declined exponentially. In cultivated sites (HS4), 94% of the ^{137}Cs was found in the top 30 cm, and it was distributed uniformly within the plough layer, ranging from 0–15 cm (45%) to 15-30 cm (48%) [70], which was lower than the activity observed in un-ploughed sites. The ^{137}Cs activity showed a distinct profile shape for the soils of the lower hillslope (HS5) (Fig. 4), in contrast to the reference site (HS1). The profile depth distribution for the soils of HS5 site revealed highest ^{137}Cs activity (10.4 Bq Kg^{-1}) at 30-50 cm, whereas it was 1.8 Bq Kg^{-1} and 3.0 Bq Kg^{-1} at 0–15 cm and 15–30 cm, respectively indicating relatively low activities and thus deposition of eroded sediments brought from upslope area. After a depth of 50 cm, the ^{137}Cs activity was quite low (0.3–1.3 Bq Kg^{-1}), clearly indicating that the 30–50 cm layer represents the buried topsoil horizon of the soils at the valley hillslope (HS5). The ^{137}Cs activity was found up to a depth of 75–100 cm increment in the lower hillslope position. Additionally, the occurrence of very intense rainfall (Supplementary Fig. 2) in the study site may contribute a significant sediment load from upslope contributing areas in a short period. Similar profile shapes were reported by Porto et al. [71] in deposition zones and in low floodplain zones [72]. Froehlich [73] also reported a similar shape of ^{137}Cs depth distribution in flood plains of North-east Himalayas at a depth between 30–50 cm.

3.4 Measurement and modelling of ^{137}Cs reference inventory

At the reference sites of Harsil (H1) hillslope, the mean value of ^{137}Cs inventories was measured at 2172.8 ± 433.1 Bq m^{-2}, with a coefficient of variation (CV) of 20% (Fig. 3). For the Gangnani (H1) hillslope, the mean value of ^{137}Cs inventories was measured at 2054.5 ± 265.20 Bq m^{-2}, with a coefficient of variation (CV) of 12.91% (Fig. 4). There has not been any study to date comparing the reference inventory for the higher Himalayas. However, some studies had been conducted in the foothill Himalayas by Mariappan et al. [40] reported a modeled inventory of 1685 Bq m^{-2} (modelled inventory-2013), and in the Meghalaya, Prokop and Poreba [9] reported a measured inventory of 1220 Bq m^{-2} (sampling year-2012), both at lower latitudes and higher longitudes compared to this study. Mandal et al. [39] conducted a study in Dehradun and found ^{137}Cs values ranging from 944 to 1170 Bq m^{-2}. Moreover, Tagami et al. [74] conducted a study to assess the spatial distribution of ^{137}Cs reference site soils in South Asia. They found that the 30–40° latitude band had a geometric mean of 1576 Bq m^{-2}, with values ranging from 860 to 3731 Bq m^{-2}. In Srinagar, Jammu and Kashmir (34.083° N), ^{137}Cs values were recorded at 2685 Bq m^{-2}, while New Delhi (28.583° N) showed 1580 Bq m^{-2} (decay corrected—2022) [74, 75]. Additionally, models were employed to verify the reliability of the reference value of ^{137}Cs inventory [9]. The scarcity of data necessitates checking the reliability of measured reference inventory against

global reference inventory models. Various models were adopted to predict ^{137}Cs fallout using monthly precipitation data from the India Meteorological Department (IMD). The models yielded a reference inventory ranging from 1606 to 2006 Bq m^{-2} (Supplementary Table 2; Supplementary Figs. 4, 5). All methods estimated inventories that were quite close in magnitude to the measured 'reference' inventories at the reference site. Any differences observed can likely be attributed to the spatio-temporal variations in rainfall across the hilly and mountainous landscape. Consequently, the observed reference inventory was considered the actual value for quantifying erosion and deposition processes.

3.5 Measurement of ^{137}Cs inventories at the hillslope positions

In the Harsil (H1) hillslope position, the activities of ^{137}Cs inventories were calculated at five hillslope positions along the transect, ranging from 1373.8 (HS2) to 3219.7 Bq m^{-2} (HS3), as depicted in Fig. 3. The ridge hillslope (HS1) exhibited a ^{137}Cs concentration of 2025.6 ± 91.7 Bq m^{-2}, whereas in the upper hillslope (HS2) covered with forest, the value was 1373.8 ± 133.1 Bq m^{-2}, while lower hillslope (HS4) recorded a ^{137}Cs inventory of 1404.3 ± 131.4 Bq m^{-2}, and HS5 had a ^{137}Cs concentration of 1649.9 ± 317.6 Bq m^{-2}. The coefficients of variation for ^{137}Cs in HS1, HS2, HS3, HS4, and HS5 were 5%, 10%, 12%, 9%, and 19%, respectively. The highest variation was observed in the valley hillslope position and deposited regions. The activities of ^{137}Cs inventories were calculated at five hillslope positions along the transect of the Gangnani (H2) hillslope. The values range from 244.2 (HS3) to 2213.0 Bq m^{-2} (HS5), as illustrated in Fig. 4. The ridge hillslope with grass and shrub cover exhibited a value of 1538.0 ± 84.6 Bq m^{-2}, upper hillslope (HS2) with forest exhibited a value of 904.1 ± 69 Bq m^{-2}, while the lowest ^{137}Cs inventory of 244.2 ± 52.1 Bq m^{-2} was found in the middle hillslope cropland (HS3). This inventory is approximately four times lower than the natural forest cover (upper hillslope-HS2). Forested soils had considerably higher values of ^{137}Cs compared to cultivated soils [76]. The ^{137}Cs inventories for croplands in HS4 and HS5 were 1185.2 ± 243.8 and 2213.0 ± 53.5 Bq m^{-2}, respectively (Fig. 4). The coefficients of variation for ^{137}Cs in HS1, HS2, HS3, HS4, and HS5 were 5.5%, 7.6%, 21.7%, 20.5%, and 2.4%, respectively. The concentration of ^{137}Cs specific activity (Bq kg^{-1}) and areal activity (Bq m^{-2}) may have varied in relation due to the presence of high coarse fragments, stones, organic matter content, and bulk density of the samples. The observed soil redistribution patterns on terraced fields align with the erosion and deposition patterns typically associated with soil erosion, as indicated by previous studies [70, 77]. Notably, in the managed site, the primary soil conservation measures focused on constructing broad-base terraces to reduce the slope length (Fig. 5). These practices have significantly altered the flow patterns, consequently impacted soil redistribution and resulting in relatively high variability in ^{137}Cs inventories. Significantly, in the managed site, the key soil conservation measures were focused on constructing broad-base terraces to diminish the slope length (Fig. 6). The undisturbed forest land exhibited low variability, while the cultivated terraced field demonstrated high variability. The entire ^{137}Cs inventory (Gangnani—H2) in the surface soil of cultivated (HS3 and HS4) and uncultivated (HS1 & HS2) sites were lower than the reference inventory, indicating net soil loss, while it was higher in valley (HS5) hillslope position, conferring the deposition of sediments. The rate of soil transport to downslope was proportionate to the slope, thus soil loss was more evident on steep slopping terraces (terrace width 6 m at HS3) and relatively less on moderate sloping terraces (terrace width 12 m at HS4) [61].

3.6 Estimation of soil redistribution rates

To determine the soil redistribution rates across different hillslope positions, we used the MODERN model. The MODERN model allows for comparison between the depth distributions of ^{137}Cs from both the reference and sampled sites. To investigate ploughing mechanisms using MODERN, we conducted simulations involving a single plough layer (typically at a depth of 15 cm) positioned above the observed depth profile. Concurrently, to explore deposition mechanisms using MODERN, we conducted simulations involving a single/double deposition layer positioned above the observed depth profile. The ^{137}Cs inventory in these simulated layers were determined based on the average value of the ^{137}Cs inventory measured in the upper horizon of the respective site assuming a variable depth distribution of ^{137}Cs with respect to disturbed sites. Thus, varying surface ^{137}Cs concentrations corresponding to the observed values were selected for each hillslope position.

3.7 Harsil (H1)

The ridge/ hill top (HS1), upper (HS2), lower (HS4), and valley (HS5) hillslope positions were assessed for net erosion rates, yielding values of − 2.9 ± 0.0, − 11.6 ± 2.0, − 15.6 ± 2.5, and − 8.9 ± 0.0 t ha^{-1} yr^{-1} respectively (Fig. 7). In HS4, the terraced

Fig. 5 Various land use/land cover under different hillslope positions of Harsil (H1) hillslope (**a**) terraced field, (**b**) deodar forest, (**c**) apple orchard (deposition), and (**d**) apple orchard (eroded)

Fig. 6 Various land use/land cover under different hillslope positions of Gangnani (H2) hillslope (**a**) grass and shrub cover, (**b**) deodar forest, (**c**) broken terraced field, (**d**) terraced mustard crop field

Fig. 7 Hillslope position-based soil redistribution rate
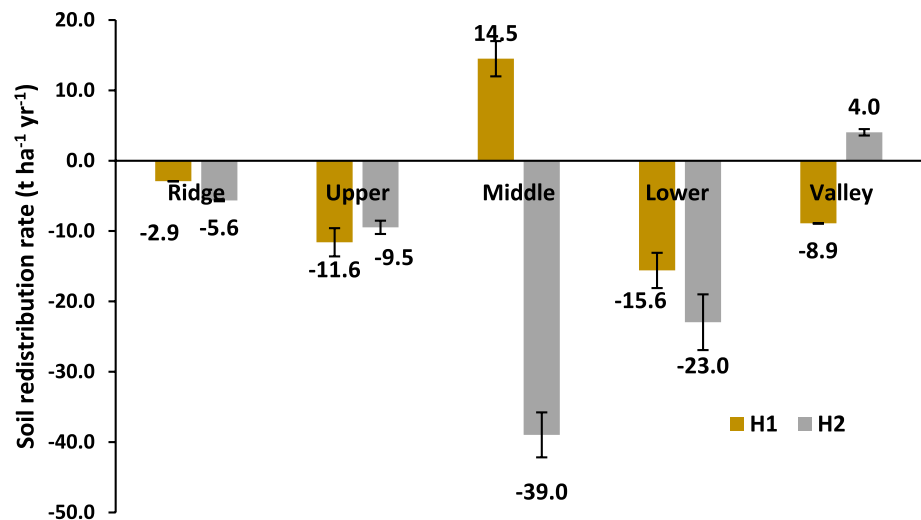
fields (width) were narrow with high riser on the steep slopes. It witnessed removal of the topsoil due to high surface runoff from the upslope areas. The average net erosion rate (for eroded areas) of the entire hillslope was determined to be − 9.75 t ha^{-1} yr^{-1} (Fig. 7). The middle hillslope (HS3) (Fig. 5 c), characterized by a concave shape with a lower slope, exhibited a deposition of 14.5 ± 2.5 t ha^{-1} yr^{-1}. At this position, the terrace fields were wide with low riser and lesser slopes, that promoted the sediment deposition from the upslope areas. The hillslope position with the highest slope (32%) was observed with the highest soil erosion (HS4), whereas flat cultivated land (2%) experienced lower soil erosion (HS1) within similar land use (Fig. 5). Additionally, the upper hillslope forest, with the highest slope (65%), observed the second-highest soil erosion rate. Conversely, the middle hillslope, with an 8% slope, experienced a net deposition of sediments from the upper slope areas. The conservation practices adopted, such as levelling terraces with stone patching on riser, provide stability to the slope and helped to prevent soil erosion (Fig. 5c, d).

Topographic factors such as slope, slope shape, and aspect were likely to exert a significant influence on the redistribution of ^{137}Cs in the landscape. Soil loss and runoff rates in croplands are known to be affected by both the slope gradient and slope length [78]. For instance, in subtropical terraced apple orchards in Spain, an erosion rate of 9.1 t ha^{-1} yr^{-1} was reported with an annual rainfall of 449 mm [79], while in our case, the rainfall is higher at 1175 mm. Kothyari et al. [80] measured the highest soil erosion rate of 5.47 t ha^{-1} yr^{-1} with a slope of 33.46% and rainfall of 179.33 mm from runoff plots in the Pine Forest of Kumaon Himalayas. Kalambukkattu et al. [8] reported soil erosion rates in evergreen and deciduous forests ranging from 10 t ha^{-1} yr^{-1}. Whereas in cultivated areas, studies by Sen et al. [81] and Semwal et al. [82] on terraced potato-cultivated slopes in the Himalayas, utilizing runoff plots, reported an average soil erosion rate of 18.5 t ha^{-1} yr^{-1}. A study on pulse crops with a 17.63% slope in the Indian Himalayas by Sen et al. [81] measured a soil erosion rate of 13.44 t ha^{-1} yr^{-1}. The accelerated soil losses 20 t ha^{-1} were recorded on outward-sloping (steep) unditched terraces in the Nepal Himalayas [83].

3.8 Gangnani (H2)

The soil erosion rates were estimated as − 5.6 ± 0.12 t ha^{-1} yr^{-1} for the ridge/hilltop (HS1) hillslope position (Fig. 6). Shrub land and grassland have the lowest erosion rates reported by Cerdan et al. [84]. The forested upper hillslope (HS2) was characterized as a very steep slope of 100–119% with net soil erosion rate of − 9.5 ± 0.2 t ha^{-1} yr^{-1} over the last six decades. Similarly, Yuan et al. [85] conducted a study using ^{137}Cs in the Nepal Himalayas the sloping forest land has a net soil erosion rate of 13.6 t ha^{-1} yr^{-1}. They suggested that increasing rainfall amount/intensity was reasoned for the soil erosion. Whereas some other studies conducted using ^{137}Cs in the Nepal Himalayas reported the soil erosion rate up to 29.63 t ha^{-1} yr^{-1} for forestland sites [65]. There were limited number of measured and calibrated studies available for comparing soil erosion in the Himalayas, and none was available for the Higher Himalayas. Kalambukkattu et al. [8] also reported a mean erosion rate of around 10 t ha^{-1} yr^{-1} from an evergreen forest using the RUSLE model. Likewise, David Raj et al. [6, 13] reported that the deciduous forest in the Shiwalik Himalayas exhibited a net erosion rate of 13.61 t ha^{-1} yr^{-1} using a gauged watershed and a calibrated APEX model. Koirala et al. [86] also reported comparatively low soil erosion from forested land. Moreover, tree roots have been found to enhance soil

water retention and mitigate the direct impact of rainfall splash [87]. Wu et al. [88] reported that forests are most effective in reducing runoff and sediment yield, particularly on slopes ranging between 36.40 to 57.73%. Forests and scrub lands, characterized by a thicker canopy and a denser layer of litter and humus, have a higher capability to dissipate rainfall and improve infiltration. This, in turn, leads to a substantial reduction in runoff. Forest has a pivotal role in regulating the interaction between slopes and soil erosion [89]. The presence of mixed dense forests with a thick grass cover on the soil surface has been effective in reducing soil erosion rates on upper hillslopes.

The soil erosion rate was estimated to be the highest, with a net soil erosion rate of -39.7 ± 1.9 t ha^{-1} yr^{-1} at the middle hillslope (HS3). At this hillslope position, terrace fields were found damaged due to severe soil erosion (Fig. 6c). It was caused by higher surface runoff from the upper slope areas as well as no stone patching on the riser of these terraced fields. This concentrated flow led to increased soil erosion and forming gullies as well. Terraces closely interconnected with one another are reinforced and shielded from collapsing by stone patching risers and mud. Consequently, if one terrace was abandoned and its riser was damaged, it increased the vulnerability of other terraces, especially during heavy rainfall, as pointed out by Maikhuri et al. [90]. It revealed a higher soil erosion from improperly managed terraced cropland. Prokop and Poreba [9] estimated that annual soil loss from cultivated fields in the North-east Himalayas ranged from 32 to 79 t ha^{-1} yr^{-1}. Similarly, Yuan et al. [85] conducted a study using ^{137}Cs in Nepal Himalayas the sloping terraced cultivated land has a mean net soil erosion rate of 32.2 t ha^{-1} yr^{-1} and they even observed upto 37.08 t ha^{-1} yr^{-1} over sloping farmland. In Nepal Himalayas Su et al. [65] reported that soil erosion rates of 70.17 t ha^{-1} yr^{-1} for terraced cultivating fields. In the cultivated region of Iran (with rainfall of 991 mm) the even high mean erosion rates up to 49 t ha^{-1} yr^{-1} observed using ^{137}Cs approach. Sooryamol et al. [91] reported 30.2 t ha^{-1} yr^{-1} of net erosion rate from terraced maize field of lesser Himalayas using gauged watershed employing SWAT model. Kalambukattu et al. [8] also reported an erosion rate of > 30 t ha^{-1} yr^{-1} from terraced cropland of Uttarakhand Himalaya using RUSLE.

The soil erosion rate was estimated to be -23.0 $\pm$ 3.1 t ha^{-1} yr^{-1} for the terraced cropland with 57.7–64.9% slope on the middle hillslope (HS4). However, in the case of the lower hillslope terraced cultivation (HS4), demonstrated relatively less soil erosion compared to HS3. These terraces are slightly outward sloping, and the absence of embankments / bunding at the edges caused soil erosion. The results regarding soil erosion from steep terraced landscapes in the Middle Mountains of Nepal surpass the observed soil erosion rates in the terraced landscape located in the upper regions of the Changjiang River (37.90 t ha^{-1} yr^{-1}) and the Yimeng Mountains (27.00 t ha^{-1} yr^{-1}) in China, as reported by Zhang et al. [92, 93]. The lower hillslope (HS4) position has a slight concave shape, resulting less erosion. The width of terraces was wider compared to those in the middle hillslope field (HS3). Additionally, the edges of the terrace risers were reinforced with stone to withstand the high surface flow originating from the upper slope areas. Farmers in this area have been using traditional tillage methods, including animal tillage, for over a century. The lower erosion rate observed employing the ^{137}Cs method suggests the beneficial effects of traditional agricultural techniques, particularly the implementation of terraces. Effective management of terrace fields by farmers has helped to reduce the soil erosion in this area. To mitigate water erosion, the hillslopes have been divided into terraces to reduce the steepness of slopes. Therefore, it is crucial to implement effective control measures for erosion management [94]. The net erosion rates decline as move downhill from middle hillslope, which signifies the downslope movement of eroded soil, its transportation, and the deposition of eroded materials [70]. The deposition was observed at the valley hillslope cropland (HS5), ranging from 4.04 $\pm$ 0.45 t ha^{-1} yr^{-1}. Hillslopes were well-managed terracess with moderate sloping lies at the lowest position receiving sediments from upslope area witnessing low erosion rate.

Several studies have identified ^{137}Cs as a reliable method for estimating soil erosion and deposition in various regions around the globe. In a study on sloping cropland, Olson et al. [95] employed both magnetic tracers and radio-cesium techniques to assess historical soil erosion rates. Their findings indicated that the combination of fly ash and cesium-137 was effective in quantifying erosion amounts and determining annual soil erosion rates across different positions on cropland landscapes. They revealed that the highest erosion rates occurred at the upper and lower backslopes of the cropland. Specifically, the annual erosion rates for the backslope during three distinct time periods were found to be 51 t ha^{-1} yr^{-1}. According to Mandal et al. [39] the effectiveness of using ^{137}Cs for estimating soil erosion was dependent on the severity of the erosion process. Nonetheless, when it was compared to traditional soil erosion assessment techniques, the ^{137}Cs method had demonstrated a highest ability to measure soil redistribution, achieving an accuracy rate between 93 and 99% in cases of severe to very severe erosion conditions [46]. This technique overcomes the limitations of conventional methods by utilizing naturally occurring radionuclides and stable isotopes as tracers, which enhanced the ability to investigate and understand the erosion processes [22]. Using the RUSLE method, erosion was found to be categorized from medium to very high, with rates varying from 1 to 33 t ha^{-1} yr^{-1}. Estimates based on ^{137}Cs have offered

a comprehensive understanding of the isotope's distribution across the slopes, reflecting erosion rates from 26 to 42 t ha^{-1} yr^{-1}, depending on the specific models applied [96].

3.9 Characterizing critical hillslope position/hotspot of soil erosion

Soil erosion is primarily linked to rainfall-runoff processes, although in mountainous areas, the process is dominantly governed by topography. The dominant soil erosion mechanism varies in each hillslope position, depending upon the interaction between major soil erosion-causing factors. In the Harsil (H1) hillslope, the highest soil erosion in the lower hillslope (HS4) might be attributed to increased snowmelt runoff from the upper slope area. The selected hillslope was affected by seasonal snowfall during winter, which often lead to soil redistribution through snow movements and melting (Fig. 8). Snowmelt runoff and snow movement-related activities may also be significant variables that could increase soil erosion [97, 98] in the hilly and mountainous regions. Thus, the erosion observed was a combination of rainfall runoff and snowmelt runoff soil erosion. Spring snowmelt runoff frequently triggered water erosion in regions where freezing temperatures and snow cover endure for months [99]. The amount of snowfall, slope gradient, land use type, and frost penetration depth all impact erosion intensity [100]. Moreover, snowmelt runoff can generate gullies, and these gullies can further extend, becoming longer, wider, and deeper. Figure 8 provides insight into how snowmelt runoff causes gully formation and subsequent erosion.

In Gangnani (H2) hillslope, the middle hillslope (HS3) stands out as the most unstable terraced cropland with the highest soil erosion rate. This was evident in the form of terraced fields with broken bunds and slanting risers (Fig. 6c), rendering it severely eroded land that serves as critical source areas for soil erosion. The soils here exhibited the lowest organic matter, indicating a high severity of soil erosion. At the onset of the rainy season, this hillslope position lacks vegetation cover and experiences splash and sheet erosion. In HS2, a high infiltration rate was induced by sandy loam soil with high porosity and organic matter content, effectively reducing surface runoff. Rainwater that infiltrates into the forested hillslope subsequently exfiltrates into the adjacent terraced fields of the hillslopes (HS3), leading to the destabilization of the risers of the terrace field and resulting in severe soil erosion (Fig. 9) [101, 102]. This hillslope position (HS3) was situated downslope of the dense forest, where concentrated surface runoff flows through gullies (Fig. 9) from the higher slope, directly inundating the bare soil surface and causing soil erosion. While the effectiveness of forests in reducing soil erosion has been established, there is a pressing need for greater efforts to sustain forests in the upslope positions of the region and to promote agroforestry systems.

Identifying soil erosion processes at the plot scale in uncontrolled plots was quite challenging due to the influence of various factors. Although FRN provided point-scale information on the dominant soil erosion processes, where it was very useful in combination with field observations to derive meaningful insights. Different soil erosion factors govern at each hillslopes and positions, including erosive agents, topography, vegetation, and upslope contributing areas. Conventional methods had serious limitations for assessing soil erosion at this scale, whereas FRN served as a suitable alternative for soil erosion measurement and interpretation. As a preliminary study in the steep-sloping hillslopes of the Himalayas, future studies may increase the number of soil sampling and sampling pattern to achieve more precise estimates. Thus, the FRN based soil erosion assessment will help to develop site-specific soil and water conservation measures for local-scale mitigation.

Fig. 8 (a) Seasonal snow-covered upper hillslope, and (b) gully formation by snowmelt runoff

Fig. 9 Thematic illustration of soil erosion processes on the typical hillslope at Gangnani
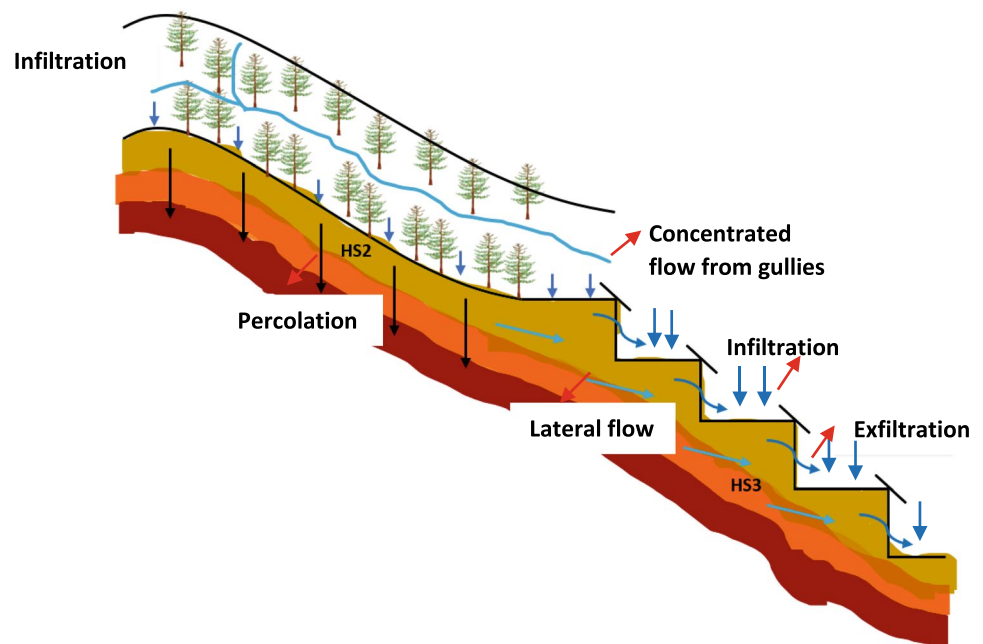
4 Conclusions

Soil erosion estimation remained a consistent concern in the hilly and mountainous regions of the Himalayas. However, assessing soil erosion in the region received relatively less attention due to the challenges posed by the region's topography and climate, which hinder the measurement of soil erosion rates. This study demonstrates the potential of using FRN (^{137}Cs) to measure soil erosion rates and identify critical soil erosion hotspots over the typical steep sloping hillslope in the Higher Himalayas. We employed fallout radionuclide (FRN) ^{137}Cs for soil erosion measurements on two typical hillslopes with mixed land use, including forest, croplands, and apple orchards.

The depth distribution analysis of ^{137}Cs revealed that the majority of ^{137}Cs was concentrated in the top 30 cm of soil, with concentrations decreasing exponentially with the depth. Our findings indicated that in the Harsil (H1) hillslope, forested area experienced lower soil erosion rate compared to orchards, while terraced fields with orchards played an important role in retaining sediments from the upslope areas, thereby preserving soils. Additionally, the slope gradient of hillslope position and snow-melt runoff were identified as a significant factors contributing to the soil erosion. In the Ganganani (H2) hillslope, cultivated terraced field exhibited very high rates of erosion, particularly those located immediately after dense forests. In steeply sloping cultivated land, these rates were four times higher than the soil erosion rates observed on very steep forested slopes, posing a significant threat to agricultural soils. The notable contrast in the average net soil erosion between cultivated and forested soils underscores that, despite the significant contribution of terraces in mitigating soil erosion in the hilly terrain, forested land remains the most effective in minimizing soil erosion in the higher Himalayas. The study confirms the effectiveness of the forest cover in conserving soils in the upslope positions of the region, suggesting that encouraging agroforestry systems could serve the dual purpose of soil conservation and meeting the needs of the farmers. Overall, it is evident that land use, combined with topography, governs the soil erosion processes and its rate at the hillslope scale.

The study also highlighted the potential of ^{137}Cs as a marker for tracing soil redistribution across the hillslope of the higher Himalayas and emphasizes the need to fully explore its potential in the region. Thus, quantifying the long-term average soil erosion processes and rates on typical hillslope positions such as ridge/ hilltop, higher, upper, middle, lower, and valley sections using FRN is necessiated. It will facilitate the identification of critical hillslope elements that require prioritization for soil and water conservation measures, and promote sustainable development of the Himalayan Mountain ecosystem. Further studies based on ^{137}Cs are needed in the Himalayan region to fully exploit its potential and improve its utilization.

Declarations

References

1. Pimentel D. Soil erosion and the threat to food security and the environment. Ecosyst Health. 2000;6(4):221–6.
2. Zhang H, Lauerwald R, Regnier P, Ciais P, Yuan W, Naipal V, et al. Simulating erosion-induced soil and carbon delivery from uplands to rivers in a global land surface model. J Adv Model Earth Syst. 2020;12(11): e2020MS002121.
3. Kohler T, Wehrli A, Jurek M, eds. 2014. Mountains and climate change: A global concern. Sustainable Mountain Development Series. Bern, Switzerland, Centre for Development and Environment (CDE), Swiss Agency for Development and Cooperation (SDC) and Geographica Bernensia. 136 pp.
4. Singh O, Singh J. Soil erosion susceptibility assessment of the lower Himachal Himalayan Watershed. J Geol Soc India. 2018;92(2):157–65.
5. Olsson L, Barbosa H, Bhadwal S, Cowie A, Delusca K, FloresRenteria D, Hermans K, Jobbagy E, Kurz W, Li D, Sonwa DJ, Stringer L. Land degradation. In IPCC special report on climate change, desertification, land degradation, sustainable land management, food security, and greenhouse gas fluxes in terrestrial ecosystems. 1. 2019. https://www.ipcc.ch/srccl/chapter/chapter-4/.
6. David Raj A, Kumar S, Regina M, Sooryamol KR, Singh AK. Calibrating APEX model for predicting surface runoff and sediment loss in a watershed—a case study in Shivalik region of India. Int J Hydrol Sci Technol. 2023;15(2):177–206.
7. Gupta S, Kumar S. Simulating climate change impact on soil erosion using RUSLE model—a case study in a watershed of mid-Himalayan landscape. J Earth Syst Sci. 2017;126:1–20.
8. Kalambukkattu JG, Kumar S, Hole RM. Geospatial modelling of soil erosion and risk assessment in Indian Himalayan region—a study of Uttarakhand state. Environ Adv. 2021;4: 100039.
9. Prokop P, Poręba GJ. Soil erosion associated with an upland farming system under population pressure in Northeast India. Land Degrad Dev. 2012;23(4):310–21.
10. Sharma PD, Goel AK, Minhas RS. Water and sediment yields into the Sutlej river from the high Himalaya. Mt Res Dev. 1991;11(2):87–100.
11. Boardman J. Soil erosion science: reflections on the limitations of current approaches. CATENA. 2006;68(2–3):73–86.
12. Borrelli P, Robinson DA, Fleischer LR, Lugato E, Ballabio C, Alewell C, Meusburger K, Modugno S, Schütt B, Ferro V, Bagarello V. An assessment of the global impact of 21st century land use change on soil erosion. Nat Commun. 2013. https://doi.org/10.1038/s41467-017-02142-7.
13. David Raj A, Kumar S, Sooryamol KR. Modelling climate change impact on soil loss and erosion vulnerability in a watershed of Shiwalik Himalayas. CATENA. 2022;1(214): 106279.
14. Ives JD, Messerli B. The Himalayan dilemma: reconciling development and conservation. London: Routledge; 1989.
15. Rana MS, Panda MR, Mehboob MS, Kim Y, Mahanta C. Understanding hydrology of Indian Himalayan Landscapes—a review. In: Dubey SK, Jha PK, Gupta PK, Nanda A, Gupta V, editors. Soil-water, agriculture, and climate change: exploring linkages. Cham: Springer International Publishing; 2022. p. 3–15. https://doi.org/10.1007/978-3-031-12059-6_1.
16. Alewell C, Borrelli P, Meusburger K, Panagos P. Using the USLE: chances, challenges and limitations of soil erosion modelling. Int Soil Water Conserv Res. 2019;7(3):203–25.

17. Froehlich W, & Walling DE. The use of^ 1^ 3^ 7Cs and^ 2^ 1^ 0Pbex to investigate sediment sources and overbank sedimentation rates in the Teesta River basin, Sikkim Himalaya, India. IAHS Publication; 2006. 306, 380.

18. Shrestha AB, Wake CP, Dibb JE, Mayewski PA. Precipitation fluctuations in the Nepal Himalaya and its vicinity and relationship with some large-scale climatology parameters. Int J Climatol. 2000;20:317–27.

19. Borrelli P, Alewell C, Alvarez P, Anache JAA, Baartman J, Ballabio C, et al. Soil erosion modelling: a global review and statistical analysis. Sci Total Environ. 2021;780: 146494.

20. Wischmeier WH, Smith DD. Predicting rainfall erosion losses. A guide to conservation planning. Agriculture Handbook n. 537, USDA, Washington, 1978. p 58.

21. Liu BY, Nearing MA, Shi PJ, Jia ZW. Slope length effects on soil loss for steep slopes. Soil Sci Soc Am J. 2000;64(5):1759–63.

22. Parwada C, Chipomho J, Tibugari H. Comparison of conventional and artificial fallout radionuclide (FRNs) methods in assessing soil erosion. Sustain Environ. 2023;9(1):2236406.

23. Kumar S, David Raj A, Mariappan S. Fallout radionuclides (FRNs) for measuring soil erosion in the Himalayan region: a versatile and potent method for steep sloping hilly and mountainous landscapes. CATENA. 2024;234(2024): 107591. https://doi.org/10.1016/j.catena.2023.107591.

24. Alewell C, Meusburger K, Juretzko G, Mabit L, Ketterer ME. Suitability of 239+ 240Pu and 137Cs as tracers for soil erosion assessment in mountain grasslands. Chemosphere. 2014;1(103):274–80.

25. Konz N, Prasuhn V, Alewell C. On the measurement of alpine soil erosion. CATENA. 2012;1(91):63–71.

26. Mabit L, Benmansour M, Walling DE. Comparative advantages and limitations of the fallout radionuclides 137Cs, 210Pbex and 7Be for assessing soil erosion and sedimentation. J Environ Radioact. 2008;99(12):1799–807.

27. Wakiyama Y, Onda Y, Mizugaki S, Asai H, Hiramatsu S. Soil erosion rates on forested mountain hillslopes estimated using 137Cs and 210Pbex. Geoderma. 2010;159(1–2):39–52.

28. Mabit L, Bernard C, Lee Zhi Yi A, Fulajtar E, Dercon G, Zaman M, Toloza A, Heng L. Promoting the use of isotopic techniques to combat soil erosion: an overview of the key role played by the SWMCN Subprogramme of the Joint FAO/IAEA Division over the last 20 years. Land Degrad Dev. 2018;29(9):3077–91.

29. Mabit L, Bernard C, Lee Zhi Yi A, Fulajtar E, Dercon G, Zaman M, et al. Promoting the use of isotopic techniques to combat soil erosion: an overview of the key role played by the SWMCN Subprogramme of the Joint FAO/IAEA Division over the last 20 years. Land Degrad Dev. 2018;29(9):3077–91.

30. Yamagata N, Matsuda S, Kodaira K. Run-off of caesium-137 and strontium-90 from rivers. Nature. 1963;200(4907):668–9.

31. Ritchie JC, McHenry JR. Application of radioactive fallout cesium-137 for measuring soil erosion and sediment accumulation rates and patterns: a review. J Environ Qual. 1990;19(2):215–33.

32. Poreba GJ. Caesium-137 as a soil erosion tracer: a review. Geochronometria. 2006;;25(37–46).

33. Arata L, Meusburger K, Frenkel E, A'Campo-Neuen A, Iurian AR, Ketterer ME, Mabit L, Alewell C. Modelling Deposition and Erosion rates with RadioNuclides (MODERN)–Part 1: a new conversion model to derive soil redistribution rates from inventories of fallout radionuclides. J Environ Radioact. 2016;1(162):45–55.

34. Khodadadi M, Alewell C, Mirzaei M, Ehssan-Malahat E, Asadzadeh F, Strauss P, Meusburger K. Understanding deforestation impacts on soil erosion rates using 137Cs, 239+ 240Pu, and 210Pbex and soil physicochemical properties in western Iran. J Environ Radioact. 2023;1(257): 107078.

35. Parsons AJ, Foster ID. What can we learn about soil erosion from the use of 137Cs? Earth Sci Rev. 2011;108(1–2):101–13.

36. Parsons AJ, Foster ID. 2013. The assumptions of science: A reply to Mabit et al. (2013). Earth-Sci Rev. 2013; 127: 308–310.

37. Zhang XJ, Zhang GH, Wei X. How to make 137Cs erosion estimation more useful: an uncertainty perspective. Geoderma. 2015;239:186–94.

38. Evrard O, Chaboche PA, Ramon R, Foucher A, Laceby JP. A global review of sediment source fingerprinting research incorporating fallout radiocesium (137Cs). Geomorphology. 2020;362: 107103.

39. Mandal D, Giri N, Srivastava P, Sah C, Bhusan R, Naregundi K, et al. 137 Cs–a potential environmental marker for assessing erosion-induced soil organic carbon loss in India. Curr Sci. 2019;117(5):865–71.

40. Mariappan S, Hartley IP, Cressey EL, Dungait JA, Quine TA. Soil burial reduces decomposition and offsets erosion-induced soil carbon losses in the Indian Himalaya. Glob Change Biol. 2022;28(4):1643–58.

41. Mariappan S, Green SM, Mishra PK, Snöälv JTC, Sharma NK, Karthikeyan K, et al. Nationwide soil erosion assessment in India using radioisotope tracers 137 Cs and 210 Pb. Curr Sci. 2018;115(3):388–90.

42. Sinha AK, Upadhyay R. Himalaya: geological aspect. J Palaeosci. 1995;44:9–28.

43. Sidhu GS, Surya JN. Soils of North-Western Himalayan eco-system and their land use, constraints, productivity potentials and future strategies. Agropedology. 2014;24(01):1–19.

44. Beck HE, Zimmermann NE, McVicar TR, Vergopolan N, Berg A, Wood EF. Present and future Köppen-Geiger climate classification maps at 1-km resolution. Sci Data. 2018;5(1):1–12.

45. Pai DS, Rajeevan M, Sreejith OP, Mukhopadhyay B, Satbha NS. Development of a new high spatial resolution (0.25× 0.25) long period (1901–2010) daily gridded rainfall data set over India and its comparison with existing data sets over the region. Mausam. 2014;65(1):1–18.

46. IAEA. Guidelines for using fallout radionuclides to assess erosion and effectiveness of soil conservation strategies (No. IAEA-TEC-DOC--1741). Joint FAO/IAEA Division of Nuclear Techniques in Food and Agriculture. 2014.

47. Mabit L, Chhem-Kieth S, Dornhofer P, Toloza A, Benmansour M, Bernard C, et al. 137 Cs: a widely used and validated medium term soil tracer. IAEA TECDOC SERIES, 27. 2014.

48. Alewell C, Meusburger K, Juretzko G, Mabit L, Ketterer ME. Suitability of 239+ 240Pu and 137Cs as tracers for soil erosion assessment in mountain grasslands. Chemosphere. 2014;103:274–80.

49. Mariappan S. Soil redistribution impacts on the spatial variation of nutrients, net carbon exchange with the atmosphere and soil respiration rates in highly eroding agricultural fields from the foothills of the Indian Himalaya. University of Exeter (United Kingdom). 2016.

○ Discover

50. Zollinger B, Alewell C, Kneisel C, Meusburger K, Brandová D, Kubik P, Schaller M, Ketterer M, Egli M. The effect of permafrost on time-split soil erosion using radionuclides (137 Cs, 239+ 240 Pu, meteoric 10 Be) and stable isotopes (δ 13 C) in the eastern Swiss Alps. J Soils Sedim. 2015;15:1400–19.

51. Loughran RJ, Wallbrink PJ, Walling DE, Appleby PG. Sampling methods. In: Zapata F, editor. Handbook for the assessment of soil erosion and sedimentation using environmental radionuclides. Dordrecht: Kluwer Academic Publishers; 2003. p. 41–57. https://doi.org/10.1007/0-306-48054-9_3.

52. Karunakara N, Chetan R, Ujwal P, Yashodhara I, Sudeep KK, Ravi PM. Soil to rice transfer factors for 226Ra, 228Ra, 210Pb, 40K and 137Cs: a study on rice grown in India. J Environ Radioact. 2013;118:80–92.

53. Pálsson SE, Howard BJ, Wright SM. Prediction of spatial variation in global fallout of 137Cs using precipitation. Sci Total Environ. 2006;367(2–3):745–56.

54. Sarmiento JL, Gwinn E. Strontium 90 fallout prediction. J Geophys Res Oceans. 1986;91(C6):7631–46.

55. Walling DE, Zhang Y, He Q. Models for converting measurements of environmental radionuclide inventories (137Cs, Excess 210Pb, and 7Be) to estimates of soil erosion and deposition rates (including software for model implementation). UK: Department of Geography University of Exeter; 2007.

56. UNSCEAR. Ionizing radiation: sources and biological effects. United Nations. 1982.

57. Walling DE, Quine T. Calibration of caesium-137 measurements to provide quantitative erosion rate data. Land Degrad Dev. 1990;2(3):161–75.

58. Shields A. Anwendung der Aehnlichkeitsmechanik und der urbulenzforschung auf die eschiebebewegung. Germany: Mitteilung der preussischen Versuchsanstalt fur Wass erbau und Schiffba Berlin; 1936.

59. Kumar A, Sharma MP, Yang T. Estimation of carbon stock for greenhouse gas emissions from hydropower reservoirs. Stochastic Environ Res Risk Assess. 2018;32(10):3183–319.

60. Rawat S, Khanduri VP, Singh B, Riyal MK, Thakur TK, Kumar M, Cabral-Pinto MM. Variation in carbon stock and soil properties in different Quercus leucotrichophora forests of Garhwal Himalaya. CATENA. 2022;213: 106210.

61. Gutiérrez-Girón A, Díaz-Pinés E, Rubio A, Gavilán RG. Both altitude and vegetation affect temperature sensitivity of soil organic matter decomposition in Mediterranean high mountain soils. Geoderma. 2015;237:1–8.

62. Conant RT, Ryan MG, Ågren GI, Birge HE, Davidson EA, Eliasson PE, Evans SE, Frey SD, Giardina CP, Hopkins FM, Hyvönen R. Temperature and soil organic matter decomposition rates–synthesis of current knowledge and a way forward. Glob Change Biol. 2011;17(11):3392–404.

63. Meusburger K, Mabit L, Park JH, Sandor T, Alewell C. Combined use of stable isotopes and fallout radionuclides as soil erosion indicators in a forested mountain site South Korea. Biogeosciences. 2013;10(8):5627–38.

64. Foucher A, Chaboche PA, Sabatier P, Evrard O. A worldwide meta-analysis (1977–2020) of sediment core dating using fallout radionuclides including 137 Cs and 210 Pb xs. Earth Syst Sci Data. 2021;13(10):4951–66.

65. Su ZA, Xiong DH, Deng W, Dong YF, Ma J, Padma CP, Gurung BS. 137 Cs tracing dynamics of soil erosion, organic carbon, and total nitrogen in terraced fields and forestland in the Middle Mountains of Nepal. J Mt Sci. 2016;13:1829–39.

66. Martinez C, Hancock GR, Kalma JD. Relationships between 137Cs and soil organic carbon (SOC) in cultivated and never-cultivated soils: an Australian example. Geoderma. 2010;158(3–4):137–47.

67. Jagercikova M, Cornu S, Le Bas C, Evrard O. Vertical distributions of 137 Cs in soils: a meta-analysis. J Soils Sedim. 2015;15:81–95.

68. Li Y, Li J, Are KS, Huang Z, Yu H, Zhang Q. Livestock grazing significantly accelerates soil erosion more than climate change in Qinghai-Tibet Plateau: evidenced from 137Cs and 210Pbex measurements. Agric Ecosyst Environ. 2019;1(285): 106643.

69. Xinbao Z, Higgitt DL, Walling DE. A preliminary assessment of the potential for using caesium-137 to estimate rates of soil erosion in the Loess Plateau of China. Hydrol Sci J. 1990;35(3):243–52.

70. Meliho M, Nouira A, Benmansour M, Boulmane M, Khattabi A, Mhammdi N, Benkdad A. Assessment of soil erosion rates in a Mediterranean cultivated and uncultivated soils using fallout 137Cs. J Environ Radioact. 2019;208: 106021.

71. Porto P, Walling DE, Callegari G. Using repeated 137 Cs and 210 Pbex measurements to establish sediment budgets for different time windows and explore the effect of connectivity on soil erosion rates in a small experimental catchment in Southern Italy. Land Degrad Dev. 2018;29(6):1819–32.

72. Mamikhin SV, Golosov VN, Paramonova TA, Shamshurina EN, Ivanov MM. Vertical distribution of 137 Cs in alluvial soils of the Lokna River floodplain (Tula oblast) long after the Chernobyl accident and its simulation. Eurasian Soil Sci. 2016;49:1432–42.

73. Froehlich WO. Soil erosion, suspended sediment sources and deposition in the Maw-Ki-Syiem drainage basin, Cherrapunji, northeastern India. IAHS Publ. 2004;288:138–46.

74. Tagami K, Tsukada H, Uchida S. Quantifying spatial distribution of 137Cs in reference site soil in Asia. CATENA. 2019;180:341–5.

75. Mishra UC, Sadasivan S. Fallout radioactivity in Indian soils. Health Phys. 1972;23(1):55–62.

76. Ayoubi S, Sadeghi N, Abbaszadeh Afshar F, Abdi MR, Zeraatpisheh M, Rodrigo-Comino J. Impacts of oak deforestation and rainfed cultivation on soil redistribution processes across hillslopes using 137Cs techniques. For Ecosyst. 2021;8(1):1–14.

77. Quine TA, Walling DE, Chakela QK, Mandiringana OT, Zhang X. Rates and patterns of tillage and water erosion on terraces and contour strips: evidence from caesium-137 measurements. CATENA. 1999;36(1–2):115–42.

78. Zhao J, Wang Z, Dong Y, Yang Z, Govers G. How soil erosion and runoff are related to land use, topography and annual precipitation: insights from a meta-analysis of erosion plots in China. Sci Total Environ. 2022;802: 149665.

79. Zuazo VD, Ruiz JA, Raya AM, Tarifa DF. Impact of erosion in the taluses of subtropical orchard terraces. Agric Ecosyst Environ. 2005;107(2–3):199–210.

80. Kothyari BP, Verma PK, Joshi BK, Kothyari UC. Rainfall–runoff-soil and nutrient loss relationships for plot size areas of Bhetagad watershed in Central Himalaya, India. J Hydrol. 2004;293(1–4):137–50.

81. Sen KK, Rao KS, Saxena KG. Soil erosion due to settled upland farming in the Himalaya: a case study in Pranmati watershed. Int J Sustain Dev World Ecol. 1997;4(1):65–74.

82. Semwal DP, Uniyal PL, Bahuguna YM, Bhatt AB. Soil Nutrient storage under different forest types in a part of central Himalayas, India. Ann For. 2009;17(1):43–52.

83. Nakarmi G, Schreier H, Merg J, Mahatma P. Erosion dynamics in the Jhikhu and Yarsha khola watershed in Nepal. In: Allen R, H Schreier, S Brown and PB Shah (eds), The people and resource dynamics project: The first three years (1996–1999). Proceedings of a Workshop held in Baoshan, China; 1999 March 2–5. Kathmandu: International Center for Integrated Mountain Development. 2000. p 209–218.

84. Cerdan O, Govers G, Le Bissonnais Y, Van Oost K, Poesen J, Saby N, Gobin A, Vacca A, Quinton J, Auerswald K, Klik A. Rates and spatial variations of soil erosion in Europe: a study based on erosion plot data. Geomorphology. 2010;122(12):167–77.

85. Yuan Y, Xiong D, Wu H, Liu L, Li W, Chidi CL, et al. Using 137 Cs and 210 Pb ex to trace soil erosion rates for a small catchment in the mid-hills of Nepal. J Soils Sedim. 2021;21:403–18.

86. Koirala P, Thakuri S, Joshi S, Chauhan R. Estimation of soil erosion in Nepal using a RUSLE modeling and geospatial tool. Geosciences. 2019;9(4):147.

87. Wittenberg L, Van der Wal H, Keesstra S, Tessler N. Post-fire management treatment effects on soil properties and burned area restoration in a wildland-urban interface Haifa fire case study. Sci Total Environ. 2020;716: 135190. https://doi.org/10.1016/j.scitotenv.2019.135190.

88. Wu GL, Liu YF, Cui Z, Liu Y, Shi ZH, Yin R, Kardol P. Trade-off between vegetation type, soil erosion control and surface water in global semi-arid regions: a meta-analysis. J Appl Ecol. 2020;57(5):875–85.

89. Jordan A, Zavala LM, Gil J. Effects of mulching on soil physical properties and runoff under semi-arid conditions in southern Spain. CATENA. 2010;81:77–85. https://doi.org/10.1016/j.catena.2010.01.007.

90. Maikhuri RK, Nautiyal A, Jha NK, Rawat LS, Maletha A, Phondani PC, et al. Socio-ecological vulnerability: assessment and coping strategy to environmental disaster in Kedarnath valley, Uttarakhand, Indian Himalayan Region. Int J Disaster Risk Reduct. 2017;25:111–24.

91. Sooryamol KR, Kumar S, Regina M, David Raj A. Modelling climate change impact on soil erosion in a watershed of north-western lesser Himalayan region. J Sediment Environ. 2022;7(2):125–46.

92. Zhang X, Walling DE, Yang Q, He X, Wen Z, Qi Y, Feng M. 137Cs budget during the period of 1960s in a small drainage basin on the Loess Plateau of China. J Environ Radioact. 2006;86(1):78–91.

93. Zhang Y, Long Y, An J, et al. Spatial patterns of Cs-137 inventories and soil erosion from earth-banked terraces in the Yimeng Mountains, China. J Environ Radioact. 2014;136:1–9. https://doi.org/10.1016/j.jenvrad.2014.04.017.

94. Rabesiranana N, Rasolonirina M, Solonjara AF, Ravoson HN, Andriambololona R, Mabit L. Assessment of soil redistribution rates by 137Cs and 210Pbex in a typical Malagasy agricultural field. J Environ Radioact. 2016;152:112–8.

95. Olson KR, Gennadiyev AN, Zhidkin AP, Markelov MV, Golosov VN, Lang JM. Use of magnetic tracer and radio-cesium methods to determine past cropland soil erosion amounts and rates. CATENA. 2013;104:103–10.

96. Badreddine B, Mohammed H, Boutkhil M, Ahmed A. Assessment of erosion: use of nuclear techniques and conventional methods—case of the Fergoug watershed, Algeria. Environ Monit Assess. 2021;193(2):55.

97. Ceaglio E, Meusburger K, Freppaz M, Zanini E, Alewell C. Estimation of soil redistribution rates due to snow cover related processes in a mountainous area (Valle d'Aosta, NW Italy). Hydrol Earth Syst Sci. 2012;16(2):517–28.

98. Konz N, Schaub M, Prasuhn V, Baenninger D, Alewell C. Cesium-137-based erosion-rate determination of a steep mountainous region. J Plant Nutr Soil Sci. 2009;172(5):615–22.

99. Ollesch G, Sukhanovski Y, Kistner I, Rode M, Meissner R. Characterization and modelling of the spatial heterogeneity of snowmelt erosion. Earth Surf Process Landforms J Br Geomorphol Res Group. 2005;30(2):197–211.

100. Komissarov M, Ogura SI. Soil erosion and radiocesium migration during the snowmelt period in grasslands and forested areas of Miyagi prefecture, Japan. Environ Monit Assess. 2020;192(9):582.

101. Navalgund RR, Senthil Kumar A, Nandy S, editors. Remote sensing of Northwest Himalayas Ecosystems. Singapore: Springer Singapore; 2019. https://doi.org/10.1007/978-981-13-2128-3.

102. Kumar S, Sterk G. Process based modeling in understanding erosion processes and soil erosion assessment at hillslope scale in the lesser Himalayas, India. In: Proceedings of the International Conference on Hydrological Perspectives for Sustainable Development, Roorkee, India, 23–25 February 2005, pp. 420–427.

Publisher's Note Springer Nature remains neutral with regard to jurisdictional claims in published maps and institutional affiliations.